

# Synthesis and Characterization of Polyimides from 4-(diphenyl phosphine oxide)phenyl Pyrromellitic Dianhydride

Yeon-Ung Bae, Tae-Ho Yoon

Department of Materials Science and Engineering, Gwangju Institute of Science and Technology, One, Oryong-dong, Buk-gu, Gwangju 500-712, Republic of Korea

Received 30 September 2010; accepted 17 May 2011

DOI 10.1002/app.34934

Published online 9 September 2011 in Wiley Online Library (wileyonlinelibrary.com).

**ABSTRACT:** A novel rigid-rod type dianhydride monomer with phosphine oxide moiety, 4-(diphenyl phosphine oxide)phenyl pyrromellitic dianhydride (POPPMDA), was synthesized via the Suzuki coupling reaction of 4-(diphenyl phosphine oxide)phenyl boronic acid (POBB) and 1-bromo-2,3,5,6-tetramethyl benzene (B4MB), followed by oxidation and cyclodehydration. The monomer was characterized by FTIR, NMR, EA, and melting point analyzer and utilized to synthesize polyimides with diamines such as bis(3-aminophenyl)phenyl phosphine oxide (*m*DAPPO) and *p*-phenylene diamine (pPDA) by varying their ratio. The polyimides were prepared via a conventional

two-step synthesis: preparation of poly(amic-acid), followed by solution imidization. The polyimides were characterized by FTIR, NMR, DSC, TGA, and TMA, and their solubility, intrinsic viscosity, and adhesive properties were also evaluated. The polyimides exhibited high  $T_g$  (342–362°C), good thermal stability (>500°C), excellent adhesive property (134–107 g/mm), and low CTE (28–17 ppm/°C). © 2011 Wiley Periodicals, Inc. *J Appl Polym Sci* 123: 3298–3308, 2012

**Key words:** polyimide; phosphine oxide; dianhydride; adhesive property; CTE

## INTRODUCTION

With microelectronic devices becoming smaller and lighter, flexible printed circuits (FPC) have been receiving increasing attention. The FPCs are, in general, made from Cu foil and polymeric films and demand that polymeric materials meet stringent requirements such as low coefficient of thermal expansion (CTE), excellent adhesion, and good solubility, in addition to high  $T_g$ , good thermal stability, low dielectric constant, and low water absorption.<sup>1–3</sup> Given such criteria, polyimides are promising candidates for FPCs due to their excellent properties,<sup>4–5</sup> but most polyimides currently available cannot satisfy such requirements.

During the past decades, considerable research have been carried out on lowering the CTE and as a result, polyimides with a CTE of  $\sim 17$  ppm/°C or lower have been prepared using rigid-rod type diamines and dianhydrides.<sup>6–8</sup> However, the insolubility of these polyimides due to their high chain rigidity has led to the use of poly(amic-acid)s to prepare poly-

meric films. This, in turn, requires the thermal conversion of poly(amic-acid)s to polyimides, a process that is accompanied by large volume shrinkage and thus large residual stress.<sup>9</sup> In addition, the polyimide films, which are laminated with Cu foils using adhesives such as acrylics, polyesters, polyamides, epoxies, and polyimides,<sup>2–3</sup> often experience adhesive failure especially at high temperatures due to their poor thermal stability.<sup>10</sup>

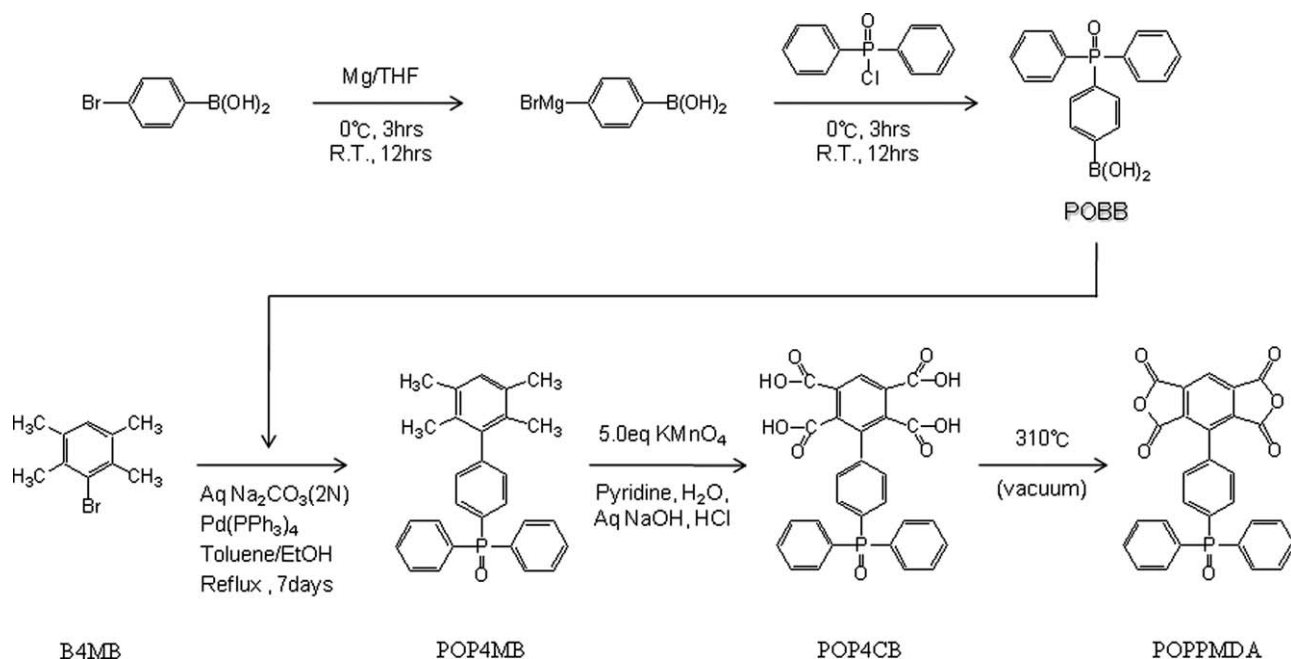
Therefore, the deposition of Cu on polyimide films via sputtering or plating<sup>11–13</sup> has been utilized to avoid the use of adhesives. Such processes, however, are known to be expensive, while poor adhesion between the polyimide film and the Cu layer poses a critical concern. Consequently, the surface modification of polyimide films, such as metal tie-layer coating,<sup>14–15</sup> plasma etching,<sup>16–18</sup> and graft polymerization,<sup>19–20</sup> has been studied. Despite some drawbacks, these processes are widely utilized in the industry, likely due to the availability of high quality polyimide films. In addition to this, the deposition of polyimides on Cu foils was also attempted.<sup>21–22</sup>

In comparison, the direct casting of polyimide solution onto the Cu foil<sup>23</sup> is a cost advantageous method, but requires soluble polyimides with low CTE and excellent adhesion. Since lowering the CTE with monomers possessing high chain rigidity is well understood,<sup>6–8</sup> and soluble polyimides can be prepared by solution or chemical imidization,<sup>24</sup> the remaining hurdle

Correspondence to: T.-H. Yoon (thyoon@gist.ac.kr).

Contract grant sponsor: National Research Foundation of Korea (NRF); contract grant number: 2004-0033933.

Contract grant sponsor: BK21 Project.



**Scheme 1** Synthetic scheme of 4-(diphenyl phosphine oxide)phenyl pyromellitic dianhydride (POPPMDA).

is improving adhesion. This can be achieved by the surface modification of Cu foil by tie-layer coating of Cr, Ti, or polymers,<sup>25–26</sup> or structural modification of polyimides with adhesion promoting groups such as pyridine<sup>27</sup> or phosphine oxide groups.<sup>28–30</sup>

However, no attempt had been made to adopt all three approaches in preparing polyimides with good solubility, low CTE, and excellent adhesion, until they were prepared from diamine containing adhesion promoting phosphine oxide groups and rigid-rod type dianhydrides via solution imidization.<sup>31–32</sup> Unfortunately, the results obtained proved to be slightly inferior for FPC application.

In this study, therefore, an attempt was made to prepare a rigid-rod type dianhydride monomer containing adhesion promoting phosphine oxide group, 4-(diphenyl phosphine oxide)phenyl pyromellitic dianhydride (POPPMDA). The monomer was combined with diamines containing adhesion promoting phosphine oxide groups such as *m*DAPPO<sup>33</sup> to provide excellent adhesion, good solubility, and low CTE. In addition, *p*PDA was also utilized to synthesize copolymers with the monomer. The polyimides were prepared via a conventional two-step synthesis; preparation of poly(amic-acid), followed by solution imidization. The prepared polyimides were characterized by FTIR, NMR, TGA, DSC, and TMA, and their solubility, intrinsic viscosity, and adhesive properties were also evaluated.

## EXPERIMENTAL

### Materials

4-Bromophenylboronic acid, Mg turning (98%), diphenyl phosphinic chloride (98%), 1-bromo-2,3,5,6-

tetramethyl-benzene (B4MB, 98%), tetrakis(triphenyl phosphine)palladium [(Pd(PPh<sub>3</sub>)<sub>4</sub>, 99.9%], and sodium carbonate (Na<sub>2</sub>CO<sub>3</sub>, 99.99%) were obtained from Aldrich and used as received. Tetrahydrofuran (THF, 99.9%, Fisher), toluene (99.9%, Fisher), 1-methyl-2-pyrrolidinone (NMP, 99.9%, Aldrich), and *o*-dichlorobenzene (*o*-DCB, 99.9%, Aldrich) were purified by distillation. The diamine monomer of bis(3-aminophenyl)phenyl phosphine oxide (*m*DAPPO) was prepared as previously reported,<sup>33</sup> while 4,4'-phenylene diamine (*p*PDA, Aldrich) and phthalic anhydride (PA, Aldrich) were used after sublimation.

### Synthesis and characterization of 4-(diphenyl phosphine oxide)phenyl pyromellitic dianhydride (POPPMDA)

A novel dianhydride monomer, POPPMDA, was synthesized via a 3-step process (Scheme 1); (1) preparation of 4-(diphenyl phosphine oxide)phenyl boronic acid (POBB), (2) Suzuki cross coupling reaction of POBB with B4MB to produce 4-(diphenyl phosphine oxide)phenyl tetramethylbenzene (POP4MB), and (3) oxidation and cyclodehydration of POP4MB to produce POPPMDA. The monomer and its intermediates were characterized by FT-IR (Shimadzu, FTIR 8400S) and NMR (JEOL, JNM-LA300WB, 300MHz) using CDCl<sub>3</sub> or deuterated dimethyl sulfoxide (DMSO-*d*<sub>6</sub>). The chemical shifts in NMR were calibrated using tetramethylsilane (<sup>1</sup>H) or phosphoric acid (<sup>31</sup>P) as the internal standard. The melting temperature was measured with a melting point apparatus (Fisher 1A9100).

### Synthesis of 4-(diphenyl phosphine oxide)phenyl boronic acid

POBB was prepared from 4-bromophenyl boronic acid and diphenyl phosphinic chloride via the Grignard reaction (Scheme 1). First, 220 mL of purified THF and 3.63 g (149.40 mmol) of Mg turning were charged into a flame-dried 500-mL three-neck round-bottomed flask equipped with a mechanical stirrer, addition funnel, drying tube, and N<sub>2</sub> inlet with attached thermometer. After cooling the mixture to ~ 0°C with an ice bath, 15.00 g (74.69 mmol) of 4-bromophenyl boronic acid was slowly added dropwise over a period of 3 h. The ice bath was then removed and the reaction mixture was allowed to react for 12 h, which resulted in a viscous dark gray solution.

Next, the solution was again cooled to ~ 0°C with an ice bath and 17.67 g (74.69 mmol) of diphenyl phosphinic chloride was added dropwise over a period of 3 h under vigorous stirring. After removing the ice bath, the mixture was further reacted for 12 h at RT, which resulted in a pale yellow solution. Finally, the solution was acidified to pH 1 with 10% aqueous sulfuric acid, and the product (POBB) was extracted by adding DI water and chloroform. The organic layer was isolated and washed with DI water several times, followed by solvent evaporation and recrystallization in chloroform to produce white crystals with 78% yield (mp: 188.6–189.3°C).

FTIR (KBr, cm<sup>-1</sup>): 3328 (O–H s), 3039 (C–H v), 1177 (P=O s).

<sup>1</sup>H-NMR (DMSO-*d*<sub>6</sub>), δ (ppm): 8.13 (s; O–H), 7.98–7.65 (m; 8H), 7.65–7.43 (m; 6H), <sup>31</sup>P-NMR (DMSO-*d*<sub>6</sub>), δ (ppm): 17.57.

### Synthesis of (4-(diphenyl phosphine oxide)phenyl)tetramethylbenzene

POP4MB was prepared from 4-(diphenyl phosphine oxide)phenyl boronic acid (POBB) and 1-bromo-2,3,5,6-tetramethylbenzene (B4MB) via the Suzuki cross coupling reaction in the presence of Pd-catalyst (Scheme 1). First, 330 mL of toluene and 13.72 g (64.38 mmol) of B4MB were charged into a 1000-mL three neck round-bottomed flask equipped with a mechanical stirrer, condenser, and N<sub>2</sub> inlet. Once B4MB was completely dissolved, 24.88 g (77.25 mmol, 20% excess) of POBB, 0.74 g (0.64 mmol, 1% of B4MB) of tetrakis(triphenyl phosphine)palladium (Pd(PPh<sub>3</sub>)<sub>4</sub>), 84 mL of aqueous Na<sub>2</sub>CO<sub>3</sub> solution (2N), and 34 mL of ethanol were added, and the mixture was refluxed for 7 days. Next, the reaction product was extracted with DI water and chloroform. The organic layer was isolated, washed with DI water several times, and condensed with a rotary

evaporator. The solid residue was recrystallized in chloroform, resulting in white crystals of POP4MB with 81% yield (mp: 213.4–214.2°C).

FTIR (KBr, cm<sup>-1</sup>): 3033 (C–H v), 2924, 2860 (C–H s), 1457, 1385 (C–H b), 1195 (P=O s).

<sup>1</sup>H-NMR (CDCl<sub>3</sub>), δ (ppm): 7.83–7.59 (m; 10H), 7.52–7.40 (m; 2H), 7.39–7.32 (t; 2H), 7.23–7.17 (d; 1H), 2.12(s; 6H) and 1.77 (s; 6H), <sup>31</sup>P-NMR (CDCl<sub>3</sub>), δ (ppm): 16.27. Elemental analysis: Calcd. for C<sub>28</sub>H<sub>27</sub>O<sub>1</sub>P<sub>1</sub> (410.48): C 81.93%, H 6.63% : Found: C 81.37%, H 6.27%.

### Synthesis of (4-(diphenyl phosphine oxide)phenyl)pyromellitic dianhydride

POP4MB was subjected to oxidation (POP4CB) followed by cyclodehydration to produce POPPMDA (Scheme 1). First, 9.3 g (22.65 mmol) of POP4MB, 400 mL of purified pyridine, and 54 mL of DI water were charged into a 1000-mL three-neck round-bottomed flask equipped with a mechanical stirrer, condenser, and N<sub>2</sub> inlet. Once POP4MB was dissolved, 17.9 g (113.28 mmol) of KMnO<sub>4</sub> was added and the mixture was refluxed for 6 h, followed by filtering and rotary evaporation. The residue was then dissolved in 400 mL of NaOH aqueous solution (4 wt %), to which 17.9 g (113.28 mmol) of KMnO<sub>4</sub> was added, and the mixture was refluxed for 2 h.

After adding dry ethanol, the solution mixture was stirred for 30 min, filtered, and condensed by rotary evaporator until the solution became saturated with the product. The solution was then acidified with aqueous HCl solution (5M) to obtain the precipitate in the form of off-white powder. After filtering and washing with DI water, the powder of (4-(diphenyl phosphine oxide)phenyl)pyromellitic acid (POP4CB) was cyclodehydrated by sublimation to obtain the pale yellow crystals of POPPMDA with 52% yield and the overall yield of 33% (mp: 325.7–326.4°C).

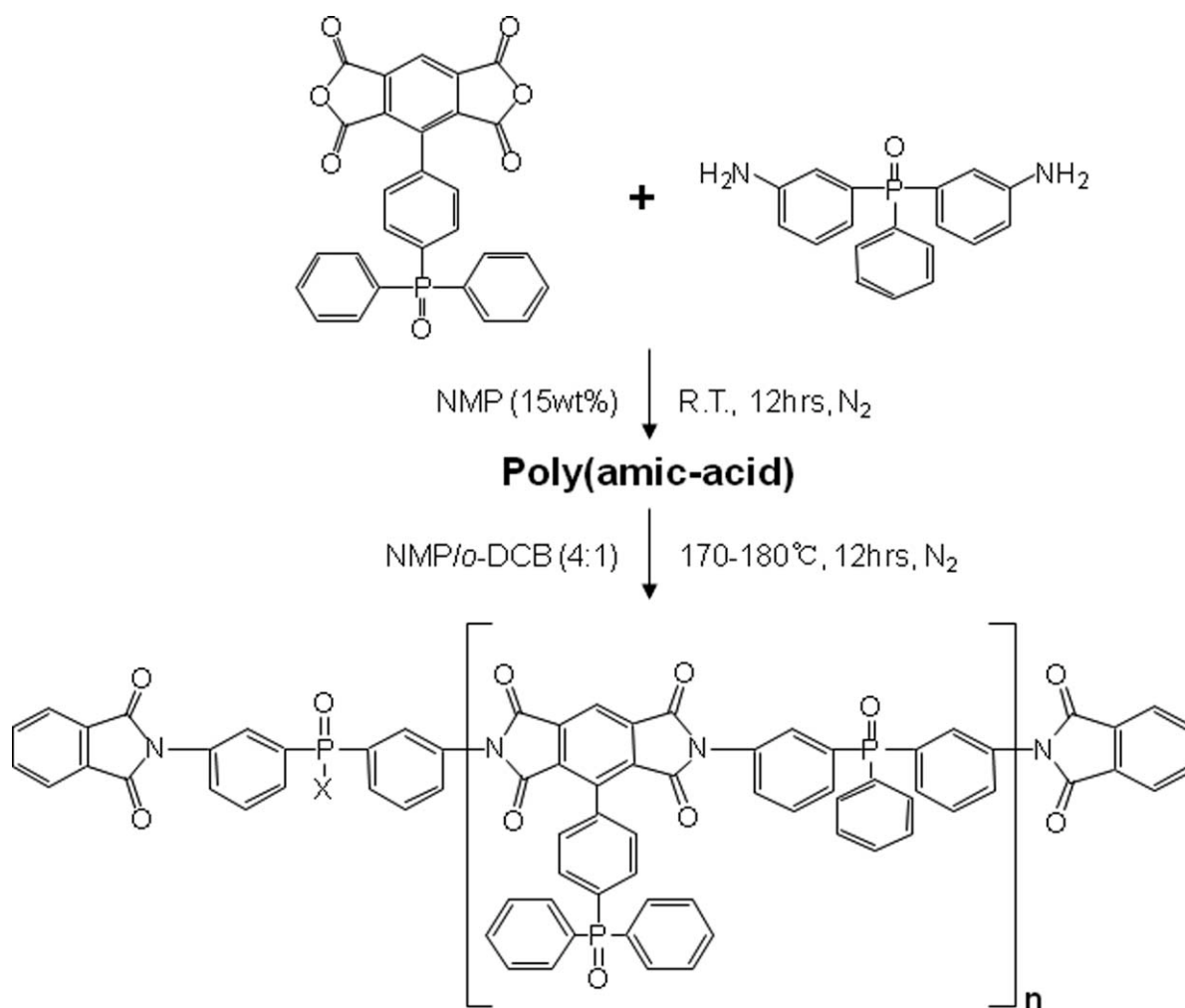
FTIR (KBr, cm<sup>-1</sup>): 3092 (C–H, v), 1870, 1784 (C=O s), 1130 (P=O s).

<sup>1</sup>H-NMR (DMSO-*d*<sub>6</sub>), δ (ppm): 8.24–7.95 (m; 3H), 7.86–7.65 (d; 2H) and 7.63–7.46 (m; 10H), <sup>31</sup>P-NMR (CDCl<sub>3</sub>), δ (ppm): 17.79. Elemental analysis: Calcd. for C<sub>28</sub>H<sub>15</sub>O<sub>7</sub>P<sub>1</sub> (494.38): C 68.02%, H 3.06% : Found: C 67.75%, H 2.73%.

### Synthesis and characterization of polyimides

#### Synthesis of polyimides

The polyimides were synthesized from POPPMDA and bis(3-aminophenyl) phenyl phosphine oxide (*m*DAPPO),<sup>33</sup> while the copolyimides were prepared by varying the molar ratio of *m*DAPPO and *p*PDA (7 : 3 or to 6 : 4) to further lower the CTE.



**Scheme 2** Synthetic scheme of polyimides with POPPMDA.

The polyimides were synthesized by a two-step process; preparation of poly(amic-acid), followed by solution imidization (Scheme 2). The number-average molecular weight ( $M_n$ ) was controlled to 35,000 g/mol by off-stoichiometry to obtain good adhesive property with reasonable melt viscosity,<sup>24</sup> and all polymers were designed to have nonreactive end groups by adding phthalic anhydride (PA).

Polymerization was carried out in a three-neck round-bottomed flask equipped with a mechanical stirrer, drying tube, nitrogen inlet, and thermometer. After flame drying under N<sub>2</sub> flow, the flask was charged with 5.000 g (16.22 mmol) of *m*DAPPO and 73 mL of dried NMP at RT. Upon complete dissolution of the diamine, 7.905 g (15.99 mmol) of POPPMDA and 0.068 g (0.46 mmol) of phthalic anhydride (PA) were added, and the mixture was reacted for 12 h to produce the poly(amic-acid) solution. Next, solution imidization was carried out at 170–180°C for 12 h under N<sub>2</sub> flow in the presence of *o*-dichlorobenzene (20 v/%) as an azeotroping agent. Finally, the reaction mixture was precipitated into a

water-methanol (1 : 1) mixture, followed by filtering and drying in a vacuum oven.

#### Characterization of polyimides

The prepared polyimides were characterized by FTIR (Shimadzu, FTIR 8400S) using KBr pellets and FT-NMR (JEOL, JNM-LA300WB) using dimethyl-*d*<sub>6</sub> sulfoxide (DMSO-*d*<sub>6</sub>), in addition to an elemental analyzer (Vario EL III). Solubility of the polyimides was evaluated in solvents such as NMP, DMAc, DMF, CHCl<sub>3</sub>, TCE, THF, and toluene at RT for 24 h at 10 wt % concentration. Since all polyimides were soluble in NMP, their intrinsic viscosity was measured in NMP at 25°C with a Cannon-Ubbelohde viscometer. Thermal properties were evaluated by DSC (TA-2910) and TGA (TA-2950) at 10°C/min. The coefficient of thermal expansion (CTE) was measured by TMA (TA-Q400) in expansion mode over the 50–250°C range at the heating rate of 5°C/min in air. The strip samples (1 × 30 mm<sup>2</sup>) were first heated to 300°C and then fast cooled to RT, followed by CTE measurement.

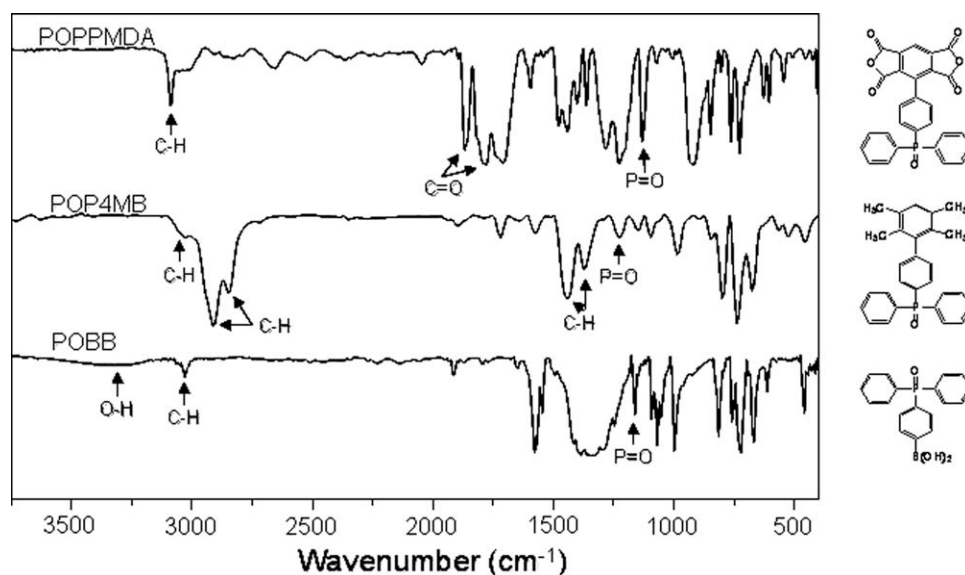


**Figure 1** FTIR of POPPMDA and its intermediate compounds.

#### Adhesive property of polyimides

The adhesive bond strength of polyimides was evaluated using modified T-peel test samples (Cu/polyimide) with Cr-silane coated Cu foils (UCF-18, 0.018-mm thick) from LS Mtron, Korea, instead of

using ASTM D-1876 T-peel test samples (Cu/polyimide/Cu), since polyimides with high  $T_g$  provided poor adhesion due to their poor flow.<sup>34</sup> The modified T-peel test samples were prepared by brush coating the Cu foil with polyimide solution (15 wt %

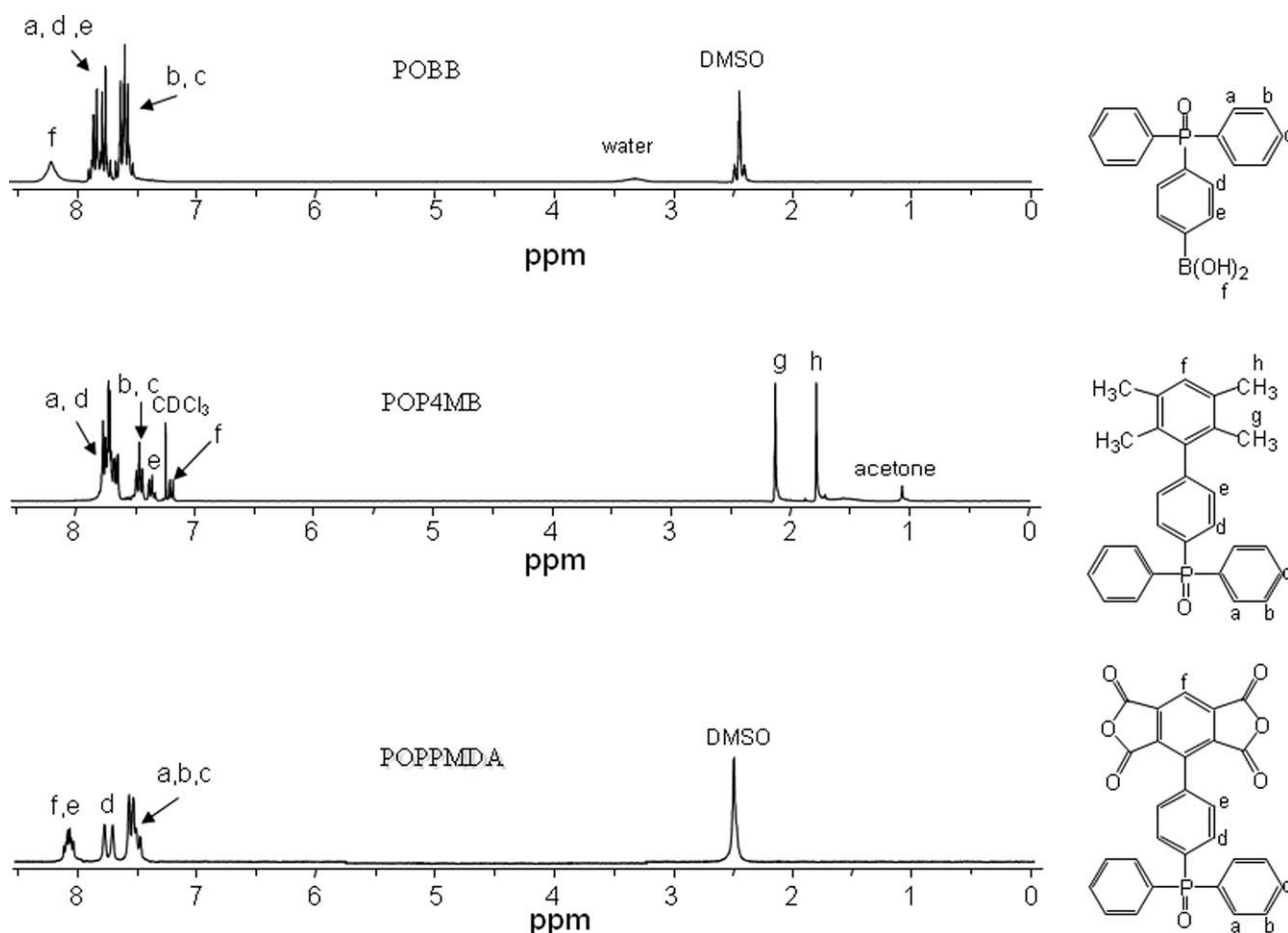


**Figure 2**  $^1\text{H-NMR}$  of POPPMDA and its intermediate compounds.

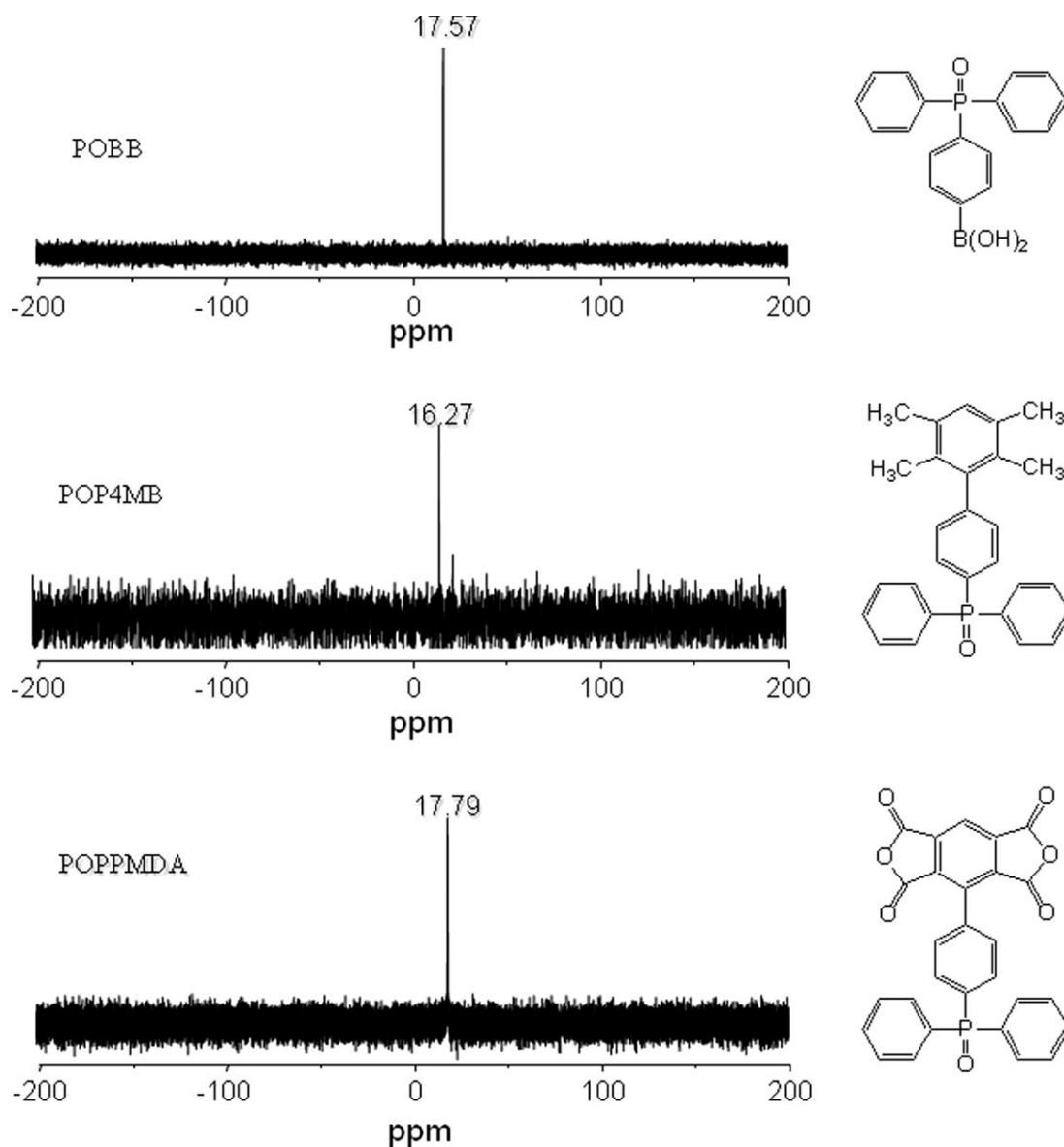


Figure 3  $^{31}\text{P}$ -NMR of POPPMDA and its intermediate compounds.

in NMP) and drying it at  $\sim 100^\circ\text{C}$  for 30 min. The process was repeated until the coating thickness reached 0.04 mm, at which time the samples were dried for 1 h each at 200 and  $280^\circ\text{C}$  and for an additional 30 min at  $350^\circ\text{C}$  under nitrogen flow to prevent the oxidation of Cu foil. Finally, the polyimide-coated Cu foil was cut into  $2 \times 150 \text{ mm}^2$  size, and its adhesive bond strength was measured by T-peel test at RT with Instron 5567 at a cross-head speed of 25.4 mm/min. The peel strength was measured from the sample mid-section (90 mm) by discarding the data obtained from 30 mm of the sample at each end. A minimum of four samples were tested and the results were averaged. Scanning Electron Microscopy (SEM, JSM-5800) was utilized to investigate the

failure mode at 15 kV and the samples were coated with gold to minimize the charging problem.

## RESULTS AND DISCUSSION

### Synthesis and characterization of POPPMDA

In the FTIR analysis, POBB exhibited the characteristic peaks of O–H stretching ( $3328 \text{ cm}^{-1}$ ), C–H vibration ( $3039 \text{ cm}^{-1}$ ) and P=O stretching ( $1177 \text{ cm}^{-1}$ ), as shown in Figure 1. Upon Suzuki cross coupling reaction of POBB with B4MB, the O–H stretching absorption ( $3329 \text{ cm}^{-1}$ ) disappeared, while new peaks corresponding to the asymmetric and symmetric C–H stretching ( $2924$ ,  $2860 \text{ cm}^{-1}$ ) and C–H bending absorption ( $1457$  and  $1385 \text{ cm}^{-1}$ ) appeared, as expected. In addition, the P=O

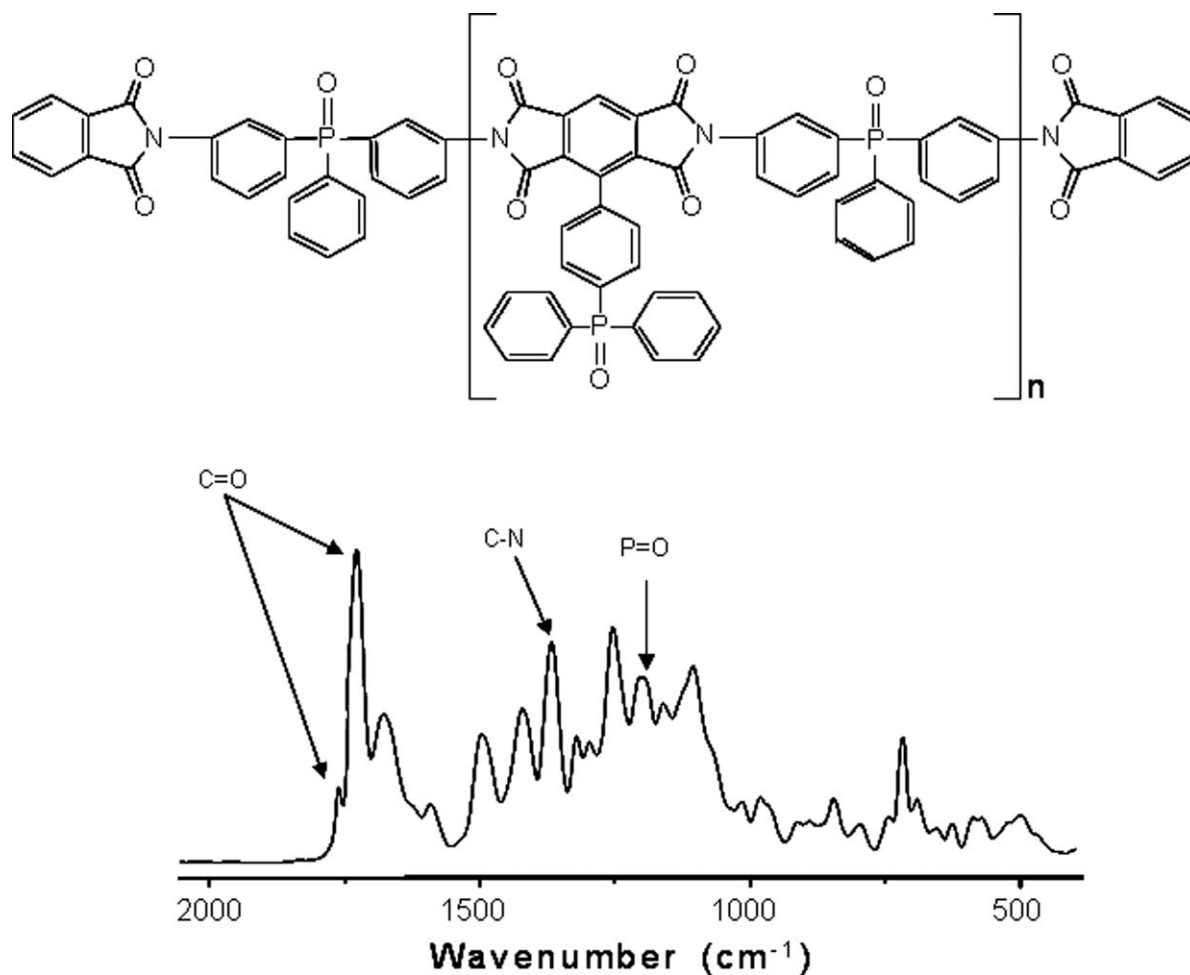


Figure 4 FT-IR of polyimide from POPPMDA-*m*DAPPO.

stretching ( $1195\text{ cm}^{-1}$ ) and C—H vibration ( $3033\text{ cm}^{-1}$ ) from the benzene ring were also observed. After oxidation and cyclodehydration, POPPMDA showed asymmetric and symmetric C=O stretching ( $1870$  and  $1784\text{ cm}^{-1}$ ) from the anhydride moieties and P=O stretching absorption ( $1130\text{ cm}^{-1}$ ) and C—H vibration ( $3092\text{ cm}^{-1}$ ) from the benzene ring, indicating a successful synthesis.

In the  $^1\text{H-NMR}$  ( $300\text{ MHz}$ ,  $\text{DMSO-}d_6$ ), POBB exhibited three groups of proton peaks at  $8.13$  (s; O—H),  $7.98$ – $7.65$  (m; 8H) and  $7.65$ – $7.43$  ppm (m; 6H) (Fig. 2) which were assigned based on the withdrawing nature of the boronic acid and the P=O group. Upon reacting with B4MB, new proton peaks were observed at  $2.12$  (s; 6H) and  $1.77$  ppm (s; 6H) arising from  $\text{CH}_3$  of POP4MB, but no peaks were observed from the boronic acid group, indicating successful Suzuki cross coupling reaction. When the cyclodehydration of POP4MB was carried out, POPPMDA exhibited three proton peaks at  $8.24$ – $7.95$ ,  $7.86$ – $7.65$ , and  $7.63$ – $7.46$  ppm, which can be assigned to the protons close to the anhydride groups (f, e), the ones between P=O and anhydride groups (d) and the ones on the phenyl ring attached to the P=O group

(a, b, c), respectively. In addition, it was noted that all peaks shifted downfield, compared to the peaks from POP4MB, demonstrating the effect of electron-withdrawing anhydride groups. In the  $^{31}\text{P-NMR}$ , a single peak was observed in all three compounds, ( $17.57$ ,  $16.27$ ,  $17.79$  ppm), indicating only one type of phosphine oxide (Fig. 3).

### Synthesis and characterization of polyimides

#### Characterization of polyimides

As shown in Figure 4, the polyimide from POPPMDA-*m*DAPPO exhibited typical imide carbonyl peaks at  $1787$  (symmetric stretching) and  $1725$  (asymmetric stretching). In addition, C-N stretching ( $1366\text{ cm}^{-1}$ ) and P=O stretching absorption ( $1183\text{ cm}^{-1}$ ) also appeared, but the amide-carbonyl (C=O) peak at  $1650\text{ cm}^{-1}$  was not observed, indicating successful imidization.

In the  $^1\text{H-NMR}$  ( $300\text{ MHz}$ ,  $\text{DMSO-}d_6$ ) of POPPMDA-*m*DAPPO, three groups of peaks were observed (Fig. 5). Considering the electron-withdrawing nature of the imide and phosphine oxide groups,

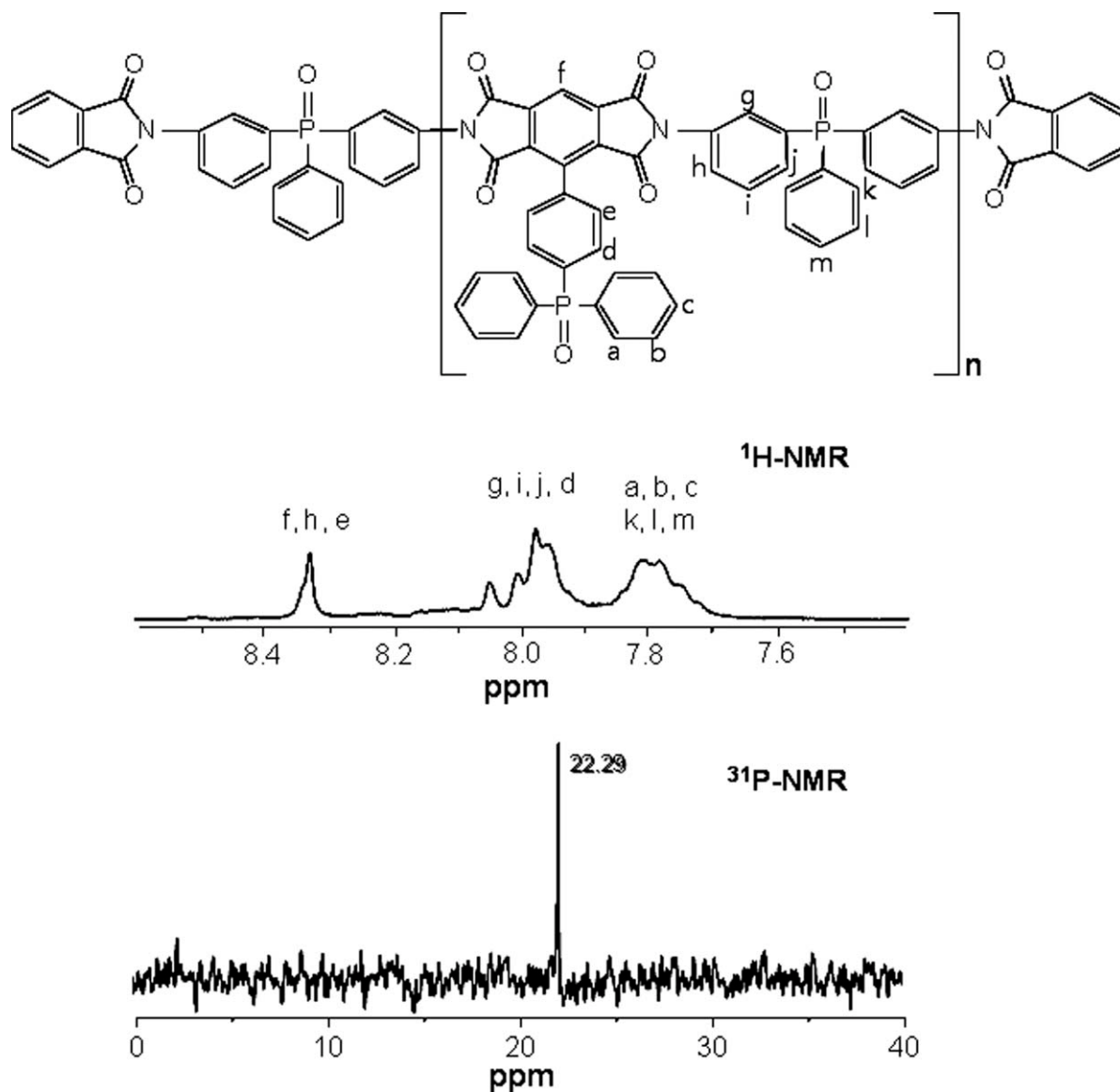


Figure 5  $^1\text{H-NMR}$  and  $^{31}\text{P-NMR}$  of polyimide from POPPMDA-*m*DAPPO.

the peak appearing far downfield ( $\sim 8.33$  ppm) is attributed to the protons between the two imide groups (f) and the ones close to the imide groups (h, e). The peak at 7.93–8.08 ppm is assigned to the protons between the imide and P=O groups (g, i, j, d), while the peak observed far upfield can be assigned to the protons on the phenyl ring, which is next to the P=O group (a, b, c, k, l, m). In the  $^{31}\text{P-NMR}$  (300 MHz,  $\text{DMSO-}d_6$ ), a single peak was observed at 22.29

ppm, indicating only one type of phosphine, possibly owing to the similar electron environment of P in the POPPMDA and *m*DAPPO moiety. The copolyimides from POPPMDA-*m*DAPPO/*p*PDA were also characterized, demonstrating successful synthesis.

#### Solubility and viscosity of polyimides

POPPMDA-based polyimides exhibited excellent solubility, as shown in Table I. The POPPMDA-

TABLE I  
Solubility of POPPMDA-Based Polyimides

Polyimide	NMP	DMSO	DMAc	DMF	$\text{CHCl}_3$	TCE	THF	Tolu
POPPMDA- <i>m</i> DAPPO	S	S	S	S	S	P	P	P
POPPMDA- <i>m</i> DAPPO/ <i>p</i> PDA (7 : 3)	S	S	S	S	P	P	I	I
POPPMDA- <i>m</i> DAPPO/ <i>p</i> PDA (6 : 4)	S	S	P	P	P	P	I	I

S, soluble; P, partially soluble; I, insoluble.



**TABLE II**  
Characteristics of POPPMDA-Based Polyimides

Polyimide	$[\eta]$ (dL/g) <sup>a</sup>	$T_g$ (°C) <sup>b</sup>	$T_d$ (°C) <sup>c</sup>	Residue (wt %) <sup>d</sup>
POPPMDA- <i>m</i> DAPPO	0.34	342	519	23
POPPMDA- <i>m</i> DAPPO/ <i>p</i> PDA (7 : 3)	0.34	355	523	20
POPPMDA- <i>m</i> DAPPO/ <i>p</i> PDA (6 : 4)	0.32	362	525	18

<sup>a</sup> At 25°C in NMP.

<sup>b</sup> By DSC, 2nd heat at 10°C/min in N<sub>2</sub>.

<sup>c</sup> By TGA, 5 wt % loss at 10°C/min in air.

<sup>d</sup> By TGA at 800°C at 10°C/min in air.

*m*DAPPO polyimide was soluble only in NMP, DMAc, DMSO, DMF, and CHCl<sub>3</sub>, while the copolymers of POPPMDA-*m*DAPPO/*p*PDA were soluble in NMP, DMAc, and DMF (7 : 3) or only in NMP (6 : 4), which is attributed to the increased chain rigidity from *p*PDA. Since all polyimides were soluble in NMP, the intrinsic viscosity was evaluated with NMP at 25°C with a Cannon-Ubbelohde viscometer. The intrinsic viscosity of POPPMDA-based polyimides ranged from 0.32 to 0.34 dL/g, indicating well-controlled molecular weights (Table II). Since all polyimide prepared in this study were insoluble in THF, the GPC analysis could not be carried out.

#### Thermal properties of polyimides

As expected, POPPMDA-based polyimides exhibited very high  $T_g$  values (342–362°C), as shown in Table II, possibly owing to the presence of rigid-rod type dianhydride. The POPPMDA-*m*DAPPO polyimide exhibited a  $T_g$  of 342°C (Fig. 6), while higher  $T_g$  values of 355 and 362°C were obtained from POPPMDA-*m*DAPPO/*p*PDA copolyimides, as expected (Table II). In the TGA analysis, all polyimides exhibited excellent thermal stability, showing 5% weight loss at temperatures above 500°C in air

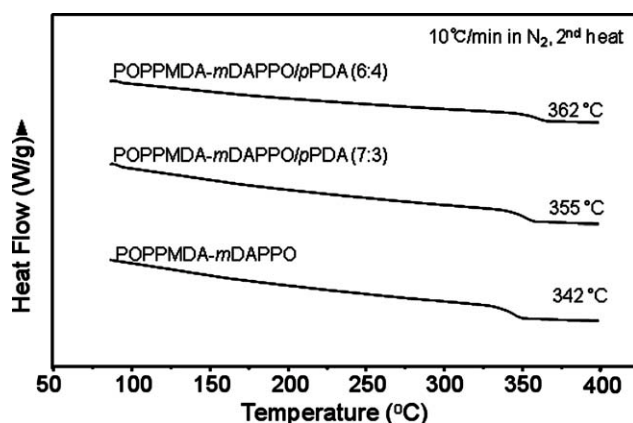


**Figure 6** DSC thermograms of POPPMDA-based polyimides.

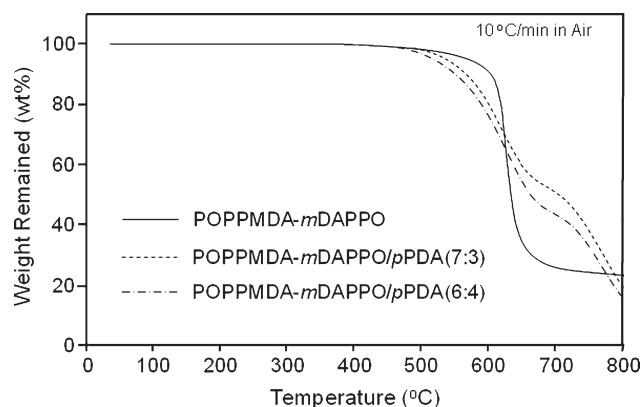


**Figure 7** TGA thermograms of POPPMDA-based polyimides in air.

(Fig. 7). In addition, the amount of residue at 800°C in air was high and correlated well to the phosphine oxide content in polyimides (Table II). In the TMA analysis, the POPPMDA-*m*DAPPO polyimide exhibited a CTE value of 28 ppm/°C, which is similar to the CTE of PI-3(30 ppm/°C) reported by Chen,<sup>6</sup> but smaller than that of Type HN polyimide film (34 ppm in 30–400°C range).<sup>35</sup> However, CTE of the POPPMDA-*m*DAPPO polyimide was still higher than that of Cu substrate (17 ppm/°C) and thus copolymerization with *p*PDA was attempted, resulting in 19 and 17 ppm/°C of CTE values, which are similar to or same as that of Cu foil (Table III).

#### Adhesive properties of polyimides

As shown in Table III, the POPPMDA-*m*DAPPO polyimide exhibited very high peel strength of 134 g/mm in the modified peel test samples (Cu/polyimide) with Cr-silane-coated Cu foil. On the other hand, the copolymers provided 115 (7 : 3) and 107 g/mm (6 : 4) which are slightly lower than that of homopolymer, attributing to the added chain rigidity from *p*PDA and the decreased P=O content in the polyimide. The peel strength of POPPMDA-*m*DAPPO polyimide can be compared to the peel strength of PPMDA-*m*DAPPO polyimide,<sup>34</sup> which

**TABLE III**  
CTE and Adhesive Properties of POPPMDA-Based Polyimides

Polyimide	CTE <sup>a</sup> (ppm/°C)	Peel Strength <sup>b</sup> (g/mm)	Failure mode <sup>c</sup>
POPPMDA- <i>m</i> DAPPO	28	134 ± 19	I
POPPMDA- <i>m</i> DAPPO/ <i>p</i> PDA (7 : 3)	19	115 ± 12	I
POPPMDA- <i>m</i> DAPPO/ <i>p</i> PDA (6 : 4)	17	107 ± 18	I

I, interfacial failure.

<sup>a</sup> By TMA, 2nd heat at 5°C/min.

<sup>b</sup> Via modified peel test samples of Cu/polyimide.

<sup>c</sup> Visual inspection.

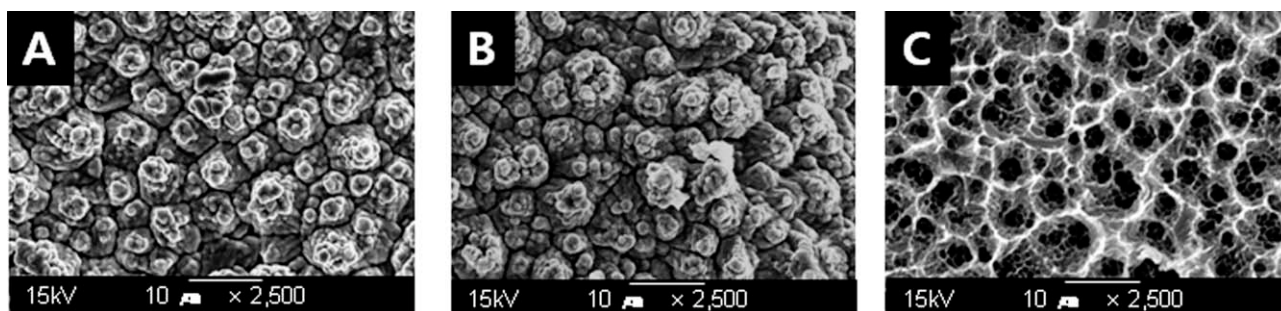


**Figure 8** SEM micrographs of fracture surface from the modified peel test samples with POPPMDA-*m*DAPPO; A) As-received Cr-silane coated Cu foil, B) Cu side, and C) polyimide side.

provided 95 g/mm with the ASTM D-1876 T-peel test samples (Cu/polyimide/Cu) and 126 g/mm with the modified T-peel samples. The results clearly demonstrate the effect of two phosphine oxide moieties in the POPPMDA-*m*DAPPO polyimide, compared to only one moiety found in PPMDA-*m*DAPPO, as well as the usefulness of the modified T-peel samples which do not require a thermal lamination process. The peel strength of POPPMDA-*m*DAPPO (134 g/mm) can be also compared with those of Pyralux® AC(119),<sup>36</sup> Pyralux® TK(124),<sup>37</sup> PI-3(128),<sup>6</sup> Pyralux® AX(137),<sup>38</sup> PI-4(160), and Pyralux® AP (160 g/mm).<sup>39</sup> These results clearly demonstrate the successful structural modification of polyimides to obtain low CTE and high peel strength.

In the SEM analysis of failure surfaces, the samples prepared with the POPPMDA-*m*DAPPO polyimide exhibited a fairly clean Cu foil side [Fig. 8(A)], similar to the as-received Cr-silane-coated Cu foil [Fig. 8(B)], with the exception that some polyimide residue remained. In contrast, the polyimide layer exhibited a sponge-like morphology [Fig. 8(C)] that matched well to the corresponding Cu foil. Thus, it can be said that failure occurred at or near the Cu/polyimide interface, although the exact failure mode needs to be determined by sophisticated surface analysis techniques. In comparison, the ASTM D-1876 T-peel test samples (Cu/polyimide/Cu) of PPMDA-*m*DAPPO polyimide showed cohesive failure, despite their lower peel strength, as previously reported.<sup>34</sup> This can be explained by the poor flow of polyimide adhesives during thermal lamination due to their high  $T_g$ , which resulted in failure occurring at the interface of two polyimide layers, despite the misleading appearance of cohesive failure.

## CONCLUSIONS

A novel rigid-rod type dianhydride monomer containing phosphine oxide moiety, POPPMDA, was successfully synthesized by the Suzuki coupling reaction, followed by oxidation and cyclodehydration. The polyimide prepared from POPPMDA and *m*DAPPO exhibited good solubility, high  $T_g$  (342°C), excellent

adhesion (134 g/mm), and good thermal stability (>500°C), but relatively large CTE (28 ppm/°C). Copolymerization [mDAPPO/*p*PDA(6 : 4)] further lowered the CTE to 17 ppm/°C, but at the expense of decreased peel strength (107 g/mm) and solubility, and increased the  $T_g$  (362°C). The excellent adhesive property of POPPMDA-*m*DAPPO polyimides can be attributed to the two P=O moieties present in the polyimides. The SEM analysis revealed that failure occurred at or near the Cu/polyimide interface, which can be attributed to the modified T-peel samples utilized in this study.

## References

1. Stearns, T. H. *Flexible Printed Circuitry*; McGraw-Hill: New York, NY, 1995.
2. Jawitz, M. W.; Jawitz, M. J. *Materials for Rigid and Flexible Printed Wiring Boards*; CRC Press: Boca Raton, FL, 2006.
3. Fjelstad, J. *Flexible Circuit Technology*, 3<sup>rd</sup> ed. B. R. Pub.; Seaside FL 2006.
4. Ghosh, M. K.; Mittal, K. L. *Polyimides: Fundamentals and Applications*; Marcel & Decker: New York, 1996.
5. Lai, J. H. *Polymers for Electronic Applications*; CRC Press: Boca Raton, FL, 1989.
6. Chen, H. L.; Ho, S. H.; Wang, T. H.; Chen, K. M.; Pan, J. P.; Liang, S. M.; Hung, A. *J Appl Polym Sci* 1994, 51, 1647.
7. Chui, C. H.; Sun, D. J.; Hsu, Y. H.; Shiang, F. T.; Chen, C. H.; Wu, P. S. C. U. S. Pat. 6,133,408 (2000).
8. Yamashita, W.; Watanabe, K.; Oquchi, T. U. S. Pat. 6,734,276 (2004).
9. Ree, M.; Nunes, T. L.; Czornyj, G.; Volksen, W. *Polymer* 1992, 33, 1228.
10. Fronz, V. *Circuit World* 1991, 17, 15.
11. Park, J. Y.; Jung, Y. S.; Cho, J.; Choi, W. K. *Appl Surf Sci* 2006, 252, 5877.
12. Hong, J. H.; Lee, Y.; Han, S.; Kim, K. *J Surf Coat Technol* 2006, 201, 197.
13. Wang, W. C.; Vora, R. H.; Kang, E. T.; Neoh, K. G. *Polym Eng Sci* 2004, 44, 362.
14. Park, I. S.; Ahn, E. C.; Yu, J.; Lee, H. Y. *Mater Sci Eng A* 2000, 282, 137.
15. Chung, Y. M.; Han, J. G. *Surf Coat Technol* 2007, 201, 5030.
16. Lin, Y. S.; Liu, H. M.; Chen, C. L. *Surf Coat Technol* 2006, 200, 3775.
17. Yang, C. H.; Lee, S. C.; Wu, J. M.; Lin, T. C. *Appl Surf Sci* 2005, 252, 1818.
18. Kim, S. H.; Na, S. W.; Lee, N. E.; Nam, Y. W.; Kim, Y. H. *Surf Coat Technol* 2005, 200, 2072.
19. Chan-Park, M. B.; Tan, S. S. *J Adhes Adhes* 2002, 22, 471.

20. Inagaki, N.; Tasaka, S.; Masumoto, M. *Macromolecules* 1996, 29, 1642.
21. Child, C. M.; Fieberg, J. E.; Campion, A. *Surf Sci* 1997, 372, L254.
22. Danev, G.; Spassova, E.; Assa, J.; Karamancheva, I.; Paskaleva, A.; Popova, K.; Ihlemann, J. *Vacuum* 2003, 70, 37.
23. Shiro, K.; Hitoshi, Y.; Souichiro, H.; Kazutsune, K. U. S. Pat. 5,112,694 (1992).
24. Arnold, C. A.; Summers, J. D.; Chen, Y. P.; Bott, R. H.; Chen, D.; McGrath, J. E. *Polymer* 1989, 30, 986.
25. Miyamura, T.; Koike, J. *Mater Sci Eng A* 2007, 445–446, 620.
26. Kim, H.; Jang, J. *Polymer* 2000, 41, 6553.
27. Ku, C. K.; Ho, C. H.; Chen, T. S.; Lee, D. *J Appl Polym Sci* 2007, 104, 2561.
28. Lee, Y. J.; Gungor, A.; Yoon, T. H.; McGrath, J. E. *J Adhes* 1995, 55, 165.
29. Jeong, K. U.; Jo, Y. J.; Yoon, T. H. *J Polym Sci Part A: Polym Chem* 2001, 39, 3335.
30. Jeong, K. U.; Kim, J. J.; Yoon, T. H. *Polymer* 2001, 42, 6019.
31. Myung, B. Y.; Kim, J. J.; Yoon, T. H. *J Polym Sci Part A: Polym Chem* 2002, 40, 4217.
32. Myung, B. Y.; Ahn, C. J.; Yoon, T. H. *Polymer* 2004, 45, 3185.
33. Martinez-Nunez, M. F.; Sekharipuram, V. N.; McGrath, J. E. *Polym Prepr* 1994, 35, 709.
34. Myung, B. Y.; Ahn, C. J.; Yoon, T. H. *J Appl Polym Sci* 2005, 96, 1801.
35. Summary of Properties for Kapton®. Polyimide Films, p. 7; Available at: [http://www2.dupont.com/Kapton/en\\_US/assets/downloads/pdf/summaryofprop.pdf](http://www2.dupont.com/Kapton/en_US/assets/downloads/pdf/summaryofprop.pdf). (2011).
36. DuPont™ Pyralux®. AC Flexible Circuit Materials; Available at: [www2.dupont.com/Pyralux/en\\_US/assets/downloads/pdf/ACclad\\_H-73247.pdf](http://www2.dupont.com/Pyralux/en_US/assets/downloads/pdf/ACclad_H-73247.pdf). (2011).
37. DuPont™ Pyralux®. TK Flexible Circuit Materials; Available at: [www2.dupont.com/Pyralux/en\\_US/assets/downloads/pdf/Pyralux\\_TK\\_DataSheet.pdf](http://www2.dupont.com/Pyralux/en_US/assets/downloads/pdf/Pyralux_TK_DataSheet.pdf). (2011).
38. DuPont™ Pyralux®. AX Copper-Clad Laminate; Available at: [www2.dupont.com/Pyralux/en\\_US/assets/downloads/pdf/AX\\_datasheet.pdf](http://www2.dupont.com/Pyralux/en_US/assets/downloads/pdf/AX_datasheet.pdf). (2011).
39. DuPont™ Pyralux®. AP All-Polyimide Flexible Laminate; Available at: [www2.dupont.com/Pyralux/en\\_US/assets/downloads/pdf/APclad\\_H-73241.pdf](http://www2.dupont.com/Pyralux/en_US/assets/downloads/pdf/APclad_H-73241.pdf). (2011).